NASA TECHNICAL NOTE

NASA TN D-2484

NASA TN D-2484

SEMICLASSICAL CALCULATION OF THE DIFFERENTIAL SCATTERING CROSS SECTION WITH CHARGE EXCHANGE:

CESIUM IONS IN CESIUM VAPOR

by John W. Sheldon

Lewis Research Center
Cleveland, Ohio

NATIONAL AERONAUTICS AND SPACE ADMINISTRATION • WASHINGTON, D. C. • SEPTEMBER 1964

SEMICLASSICAL CALCULATION OF THE DIFFERENTIAL SCATTERING CROSS SECTION WITH CHARGE EXCHANGE: CESIUM IONS IN CESIUM VAPOR

By John W. Sheldon

Lewis Research Center
Cleveland, Ohio

NATIONAL AERONAUTICS AND SPACE ADMINISTRATION

For sale by the Office of Technical Services, Department of Commerce,
Washington, D.C. 20230 -- Price $1.00

SEMICLASSICAL CALCULATION OF THE DIFFERENTIAL SCATTERING CROSS SECTION WITH CHARGE EXCHANGE: CESIUM IONS IN CESIUM VAPOR[1]

by John W. Sheldon

Lewis Research Center

SUMMARY

The differential scattering cross section of an ion in its parent gas is calculated for an inverse fourth attractive (polarization) potential. The effect of charge exchange is included. The ion and atom paths during collision are computed classically, but the results of quantum mechanical charge exchange probability calculations are used. Expressions are given for the range of energy and scattering angle over which this semiclassical approach is valid.

The differential cross section is shown to have a maximum near an apparent scattering angle of 180°. Approximate expressions are given for the value of the cross section at the maximum and the scattering angle at which it occurs.

Values of the differential cross section for cesium ions in cesium vapor are obtained by using the results of total charge exchange cross section and atomic polarizability measurements. These calculations are expected to be valid for cesium ion-atom collision energies between 0.025 and 1000 electron volts.

The relation between total cross section, charge exchange cross section, and diffusion cross section is discussed. The determination of the total cross section from a scattering chamber type experiment is presented and compared with experiments.

INTRODUCTION

Ion-Atom Resonance Charge Exchange Interaction

An ion following an interatomic path past an atom is subject to the phenomenon of charge transfer as well as scattering due to electronic interaction

---

[1]The information presented herein was offered as a thesis in partial fulfillment of the requirements for the degree of Doctor of Philosophy in Nuclear Engineering, Texas A & M University, College Station, Texas, 1964.

potentials. If the ion and atom are of identical elements, an outer electron of the atom will "see" a vacancy in the same energy level it occupies in the precollision atom. Since the probability of electron transition is inversely proportional to the difference in energy level (ref. 1), identical levels have an especially high probability of producing electron transitions. Such transitions are referred to as resonance charge exchange interactions.[2]

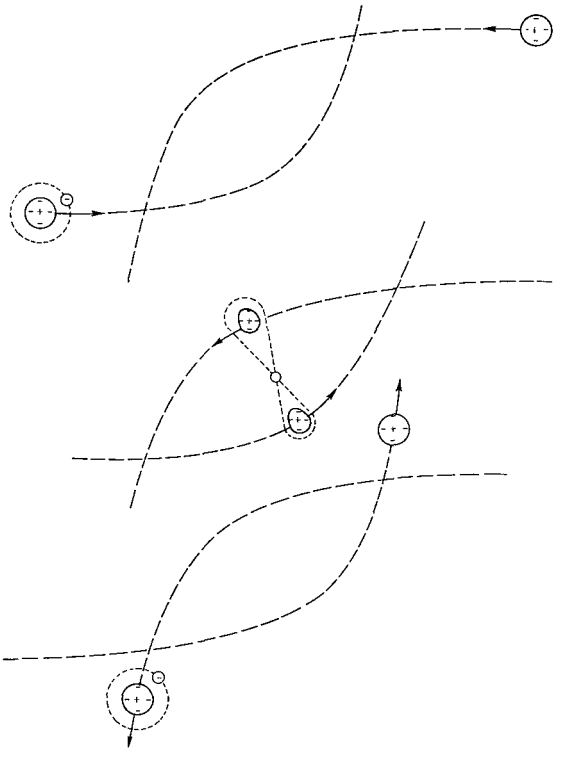

Figure 1. - Ion-neutral elastic scattering event with charge exchange.

The paths that the ion and atom follow during an interaction are determined by the influence of the electric field of one on the path of the other. For example, the electric field of the ion polarizes the atom. The induced atomic dipole then exerts an attractive force on the ion. As the distance of closest approach decreases, higher order induced field effects become significant. The deflection of the ion and atom paths during collision is referred to as elastic scattering.

An elastic scattering event with charge exchange is pictured in figure 1. If we assume the change in mass of a scattered particle (ion or atom) when an electron is gained or lost has a negligible effect on the particle kinetic energy, then the collision is experimentally identical to elastic scattering with an apparent scattering angle 180° greater than the actual particle scattering angle. Since elastic scattering is predominantly over small angles, elastic scattering with charge exchange appears to be predominantly over near-180° angles (refs. 2 and 3).

Importance of Resonance Charge Exchange Phenomena

The large apparent scattering angles that occur when ions pass through their own vapor provide an efficient mechanism for exchange of kinetic energy of the charged particles to the gas atoms, that is, to "thermalize" the field accelerated ions. This phenomenon is of current interest in connection with several thermal plasma devices. Charge exchange enhances ion neutralization of electron space charge in thermionic diode energy converters (refs. 4 to 6). Ions that have undergone charge exchange in the exhaust of an ion rocket engine have been shown to be detrimental to engine accelerator plates. An electron-

[2]Russian-to-English translators who are unfamiliar with collision phenomena often translate the Russian word for charge exchange, perezariadka, as overcharge.

bombardment ion rocket will always have some nonionized propellant flowing through the accelerator grid. These neutral atoms exchange charge with the fast moving ions in the rocket exhaust. The slow ions formed in this exchange are accelerated back into the accelerator grid where they do sputtering damage (ref. 7). Charge exchange collisions have been used in molecular beam work to produce high energy neutral beams (ref. 8).

Previous Work

There appears to have been very little work done on calculating differential scattering cross sections including elastic scattering and charge exchange. A short, qualitative discussion of the subject is given in reference 1, where it is stated that, in general, the differential scattering cross section has a large maximum at zero angle (center-of-mass system) and falls rapidly to a very small value. This small value is maintained up to an angle near 180°, after which, for resonance charge exchange, the cross section increases to a second maximum. The first maximum is attributed to direct elastic scattering, the second to elastic scattering with charge transfer. Mason and Vanderslice (ref. 9) propose a method for extending their elastic scattering cross section calculations to include charge exchange effects. There is, however, a considerable amount of literature in two closely related areas: classical calculation of elastic scattering cross section and the determination of the total charge exchange cross section.

Elastic scattering cross section. - The calculation of differential cross section due to elastic scattering reduces to the problem of solving the classical orbital equation (ref. 10) for an assumed interaction potential and then being able to differentiate the result with respect to impact parameter.

It is convenient, though arbitrary, to consider interatomic potentials to consist of two types, long and short range potentials. Short range potentials are repulsive, the result of overlap of the electron clouds. The long range potentials are attractive, the result of charge induced electrostatic multipoles and multipole induced electrostatic multipoles. An ion-atom interaction potential consisting of the following three terms is used in reference 11:

(1) An attractive potential varying as the inverse fourth power of distance that accounts for the interaction of the induced atomic dipole with the ion

(2) An attractive potential varying as the inverse sixth power of distance that accounts for two effects, the interaction of the induced atomic quadrupole with the ion and the interaction of the induced atomic dipole with the induced ionic dipole[3]

(3) A semihard sphere repulsion potential

[3]This dipole-dipole contribution to the inverse sixth power potential is often called the London dispersion potential.

Terms (1) and (2) are the leading terms in the multipole expansion. Term (3) is most often represented in the current literature by a potential varying as the inverse twelfth power of distance (refs. 9, 11, and 12). The choice of the inverse twelfth power is primarily one of mathematical convenience.

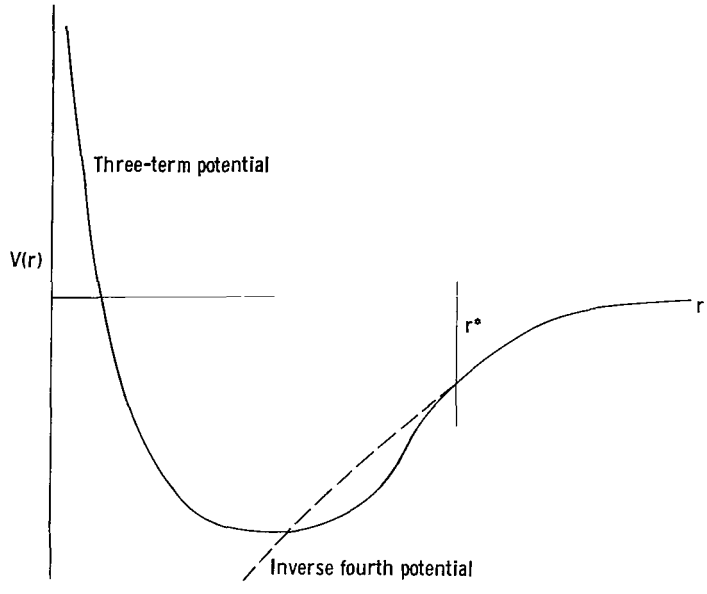

Figure 2. - Interatomic potential.

A potential consisting of these three terms is sketched in figure 2. When the relative kinetic energy of the two colliding particles is decreased, their minimum distance of approach increases. For sufficiently low energy where the minimum distance of approach is of the order of r^* (fig. 2) the more accurate three-term potential may be approximated by the inverse fourth potential alone (ref. 9). The details of particle paths followed during a polarization interaction have been discussed in references 13 and 14; however, neither reference presents an expression for the differential cross section per se.

Total charge exchange cross section. - Reviews of total charge exchange cross section data are available in standard texts (refs. 1, 3, 15, and 16). A comprehensive survey of charge exchange data was published in tabular form by Stanford University in January 1961 (ref. 17). There are no data reported below 2 electron volts.

Most of the work with cesium ions in cesium vapor, which is of special interest here, has become available since January 1961 (refs. 18 to 23). The lowest collision energy investigated is 6 electron volts (ref. 23).

The total charge exchange cross section theory may be classified by the relative velocity range over which it is applicable. The relative velocity may be considered in two ranges: high, where the relative velocity is greater than the velocity of the orbiting electron to be exchanged and low, where the relative velocity is less than the velocity of the orbiting electron to be exchanged. The work presented in this report is only applicable to the low range.

There are several theoretical treatments of low velocity charge exchange collisions. These are, with some ambiguity,[4] designated in the literature as the impact parameter method, the adiabatic method, and the perturbed stationary

[4]In reference 24 the approach is referred to as the adiabatic method; in reference 25 it is called the impact parameter method; the methods used in these two sources are identical.

state method. Actually all of these methods require the assumption of an adiabatic collision. Their main difference is the type of expansion used for the total wave function of the colliding system. Mott (ref. 26) and Demkov (ref. 27) expand the system wave function in terms of the atomic wave functions. The method of Firsov (ref. 24) and Holstein (ref. 25)[5] expands the system wave function in terms of symmetric and antisymmetric combinations of the atomic wave functions. The perturbed stationary state method introduced by Massey and Smith (ref. 28) has been presented in detail by Bates, et al. (ref. 29) who show its relation to Mott's method. Dalgarno and McDowell (ref. 30) apply the perturbed stationary state method to the calculation of total resonant charge transfer cross sections of negative hydrogen ions in atomic hydrogen. Iovitsu and Ionescu-Pallas (ref. 31) apply it to the resonant charge exchange of hydrogen-like atoms and ions. In perturbed stationary state calculations, the total system wave functions are expanded in terms of the molecular ion wave functions. Demkov (ref. 27) contends that unless the molecular ion wave functions are accurately known, the complex calculations that this treatment requires are not justified.

Present Calculation

This report combines calculations of classical low velocity elastic scattering with the quantum mechanical calculation of charge exchange probability during a low velocity collision to obtain an expression for the low velocity differential scattering cross sections with charge exchange. Experimentally determined total charge exchange cross sections (ref. 19) and atomic polarizability (ref. 32) are used in this expression to back-calculate the cesium ion-atom differential charge exchange cross sections.

The experiment of reference 19 consisted of focusing an accelerated ion beam into a charge exchange chamber. This chamber contained neutral cesium atoms (at a pressure of 0.01 to 0.1 mm of Hg) whose number density was determined by a surface ionization detector. The slow ions formed in the chamber by charge exchange were collected on parallel plates in the charge exchange chamber. The plates were at sufficiently high negative potential to collect the charge exchanged ions, but sufficiently low potential to avoid perturbing the ion beam path. This procedure restricted the experiment to beam energies above 50 electron volts. The measurement of ion beam current entering the charge exchange chamber, the current collected on the negative plates, the neutral cesium number density, and the dimensions of the apparatus allowed determination of the energy dependent charge exchange cross section for the energy range 50 to 4000 electron volts. These cross section data were compared with the theory of reference 27 in order to obtain values of exchange parameters for cesium. These same parameters appear in the differential charge exchange cross section theory.

The expression for differential scattering cross section is integrated to obtain both total and diffusion cross sections. The use of these results in

[5]Holstein (ref. 25), who published in 1952, was apparently unaware of Firsov's identical approach (ref. 24) to the problem published in Russian a year earlier.

the interpretation of low velocity scattering experiments is discussed. Interpretation of such experiments is complicated by the sizable portion of collision velocity associated with the random motion of the gas in the scattering chamber.

RESONANCE CHARGE EXCHANGE PROBABILITY

A frequently referenced theory of charge exchange probability is that presented in reference 27. This theory will be outlined here, as it allows determination of the dependence of charge exchange probability on impact parameter, a result that will be needed in later sections.

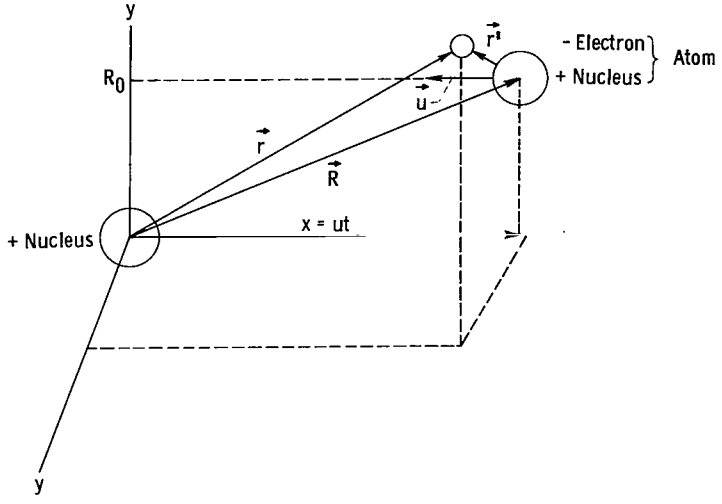

Figure 3. - Coordinate system for impact parameter treatment of resonance charge exchange.

In this treatment, an atom is considered, denoted by the subscript a, to move past an ion, denoted by the subscript i. The motion of the atom is along a straight line path in the x,y-plane of figure 3, with velocity u and closest distance of approach R_0. The ion is fixed at the origin of this coordinate system. The atom is considered as the combination of an electron and a positive nucleus or ion core. The ion at the origin is a positive nucleus of identical structure. It should be noted that the impact parameter is equal to the closest distance of approach for the special case of a straight line path. If $U_i(r)$ and $U_a(r')$ are the potential energies of the electron in the field of the ion and atom, respectively, and ψ is the time dependent wave function for the ion-atom system, the Schrödinger equation for the electron in this system is

$$\left[-\frac{\hbar^2}{2m_e}\nabla^2 + U_i(r) + U_a(r')\right]\psi = i\hbar\frac{\partial\psi}{\partial t} \tag{1}$$

where $\hbar$ is Planck's constant, h, divided by 2π, ∇^2 is the Laplacian operator, m_e is the electron mass, and t is the time coordinate, which ranges from $-\infty$ before the collision through the condition $R = R_0$ at $t = 0$ to $+\infty$ after the collision.

The total wave function must have the asymptotic form

$$\psi(t = -\infty) = \psi_0(r')e^{-\frac{i}{\hbar}m_e u x_e - \frac{i}{\hbar}\left(E_0 + \frac{m_e u^2}{2}\right)t} \tag{2}$$

where $\psi_0(r')$ is the ground-state wave function for the electron associated with the atom prior to the collision; $e^{-\frac{i}{\hbar} m_e u x}$ represents the electron motion with the incoming atom as an incoming (left running) plane wave, and $e^{-\frac{i}{\hbar}\left(E_0+\frac{m_e u^2}{2}\right)t}$ is the phase factor that contains the internal energy of the atomic system E_0 plus the kinetic energy $m_e u^2/2$.

In order to obtain $\psi(t)$ at times later than $-\infty$ out to $+\infty$ it is expanded in terms of $\varphi_n(r)$, the wave functions for the electron in the field of the ion. Hence,

$$\psi(t) = \sum_{n=0}^{\infty} a_n(t)\varphi_n(r)e^{-\frac{i}{\hbar}\epsilon_n t} \qquad (3)$$

with $\varphi_n(r)$ satisfying

$$\left[-\frac{\hbar^2}{2m_e}\nabla^2 + U_i(r)\right]\varphi_n(r) = \epsilon_n\varphi_n(r) \qquad (4)$$

The probability P_n of the electron being associated with the original ionic nucleus in the n^{th} state at $t = +\infty$ is then

$$P_n = \left|\int_{\text{all space}} \psi(+\infty)\varphi_n^*(r)d\tau\right|^2 \qquad (5)$$

where $d\tau$ is the differential volume element. Using equation (3) and orthogonality and normalization of $\varphi_n(r)$ gives

$$P_n = |a_n(+\infty)|^2 \qquad (6)$$

Substituting equation (3) into (1) and operating through with $\int\varphi_m^*(r)d\tau$ (superscript * indicates the complex conjugate) give the set of coupled simultaneous differential equations

$$i\hbar\frac{da_m(t)}{dt} = e^{\frac{i}{\hbar}\epsilon_m t}\int_{\text{all space}}\varphi_m^*(r)U_a(r')\psi(r,t)d\tau \qquad (7)$$

which may be integrated to give the coupled integral equations

$$i\hbar\left[a_m(+\infty) - a_m(-\infty)\right] = \int_{-\infty}^{\infty}\int_{\text{all space}}\varphi_m^*(r)U_A(r')\psi(r,t)e^{\frac{i}{\hbar}\epsilon_m t}\,d\tau\,dt \qquad (8)$$

Using equation (6) and the initial condition $a_m(-\infty) = 0$ yields

$$P_n = \left| \frac{i}{\hbar} \int_{-\infty}^{\infty} \int_{\text{all space}} \varphi_n^*(r) U_A(r') \psi(r,t) e^{\frac{i}{\hbar} \epsilon_n t} \, d\tau \, dt \right|^2 \tag{9}$$

Determination of P_n to a first-order approximation can be accomplished by setting

$$\psi(r,t) \simeq \psi(r,-\infty) = \psi_0(r') e^{-\frac{i}{\hbar} m_e u x} e^{-\frac{i}{\hbar}\left(E_0 + \frac{m_e u^2}{2}\right)t} \tag{10}$$

This approximation should be good for

$$P_n \leq \frac{1}{2}$$

since it assumes that the total system wave function undergoes very little change during the collision. Now for charge transfer to the ground state where both nuclei are the same element ($E_0 - \epsilon_0 = 0$), we have

$$P_0 = \left| \frac{i}{\hbar} \int_{-\infty}^{\infty} \left[\int_{\text{all space}} \varphi_0^*(r) U_A(r') \psi_0(r') e^{-\frac{i}{\hbar} m_e u x} \, d\tau \right] e^{-\frac{i}{\hbar} \frac{m_e u^2}{2} t} \, dt \right|^2 \tag{11}$$

In order to simplify integration, further approximations are made in reference 27, namely,

$$e^{-i \frac{m_e u x}{\hbar}} \simeq 1 \tag{12}$$

$$e^{-\frac{i}{\hbar} \frac{m_e u^2}{2} t} \simeq 1 \tag{13}$$

Since the remainder of the integral vanishes for large distance of separation R, we are only concerned with the validity of the preceding approximations within some interaction distance D and the corresponding time required to pass through this region T, ($T = 2D/u$). Hence, approximations (12) and (13) are equivalent and require

$$\frac{m_e u D}{\hbar} \ll 1$$

Using approximations (12) and (13) reduces the expression for charge exchange probability to

$$P_0 = \left| \frac{i}{\hbar} \int_{-\infty}^{\infty} \left[\int_{\text{all space}} \varphi_0^*(r) U_A(r') \psi_0(r') d\tau \right] dt \right|^2 \tag{14}$$

The indicated integration can be carried out for normalized hydrogen-like wave functions

$$\varphi_0(r) = \sqrt{\frac{z^3}{\pi a^3}}\, e^{-\frac{z}{a} r} \tag{15}$$

where z and a are the effective charge and effective radius, respectively, giving (see appendix)

$$P_0 = \left(\frac{e^2}{\hbar u}\right)^2 2\pi z\rho(\rho + 2)^2 e^{-2\rho} \tag{16}$$

where $\rho = zR_0/a$. Following reference 27, we can use the approximate expression for large ρ

$$P \simeq \frac{\frac{1}{2} K_1}{\epsilon}\, e^{-K_2 R_0} \tag{17}$$

where K_1 and K_2 are constants dependent on the ion and atom atomic structure and ϵ is the kinetic energy of the atom relative to the ion. Hence, the closest approach of the atom to the ion for which the exchange probability is 1/2, $R_{0,c}$, can be written

$$R_{0,c} = \left(\frac{2}{\pi}\right)^{1/2} (A - B \ln \epsilon) \tag{18}$$

where A and B are conveniently chosen new constants.

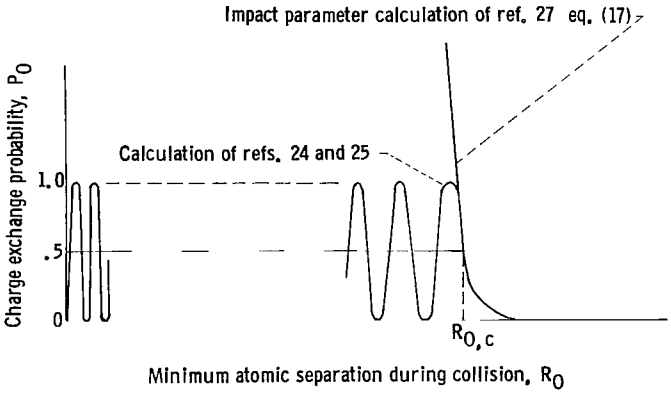

Figure 4. - Resonance charge exchange probability.

The significance of $R_{0,c}$ is evident if we look at the sketch of equation (17) in figure 4. The exchange probability obtained by Firsov (ref. 24) and Holstein (ref. 25) is also shown in this figure. Their expression is valid at small values of R_0 (where eq. (17) would give the absurd result $P_0 > 1$), and their work indicates that the average value of P_0 for $R_0 < R_{0,c}$ is 1/2; therefore, the expression

$$P_0 = \frac{1}{2} \qquad R_0 \leq R_{0,c}$$
$$P_0 = 0 \qquad R_0 > R_{0,c} \tag{19}$$

will be used, where $R_{0,c}$ is given by equation (18).

SEMICLASSICAL DIFFERENTIAL SCATTERING CROSS SECTION

Procedure

The suggestion of Mason and Vanderslice (ref. 9) can be followed to compute the differential charge exchange cross section $\sigma_x(\epsilon,\theta)$ (θ is the apparent scattering angle in the center-of-mass system; see fig. 5) by treating the particle orbit classically and the charge exchange probability P_0 by the impact parameter method. Then

$$\sigma_x(\epsilon,\theta) = P_0\sigma(\epsilon,\pi - \theta) \tag{20}$$

where $\sigma(\epsilon,\theta)$ is the classical elastic scattering cross section and θ is the apparent scattering angle in the center-of-mass system. The actual elastic scattering cross section $\sigma_e(\epsilon,\theta)$ is then

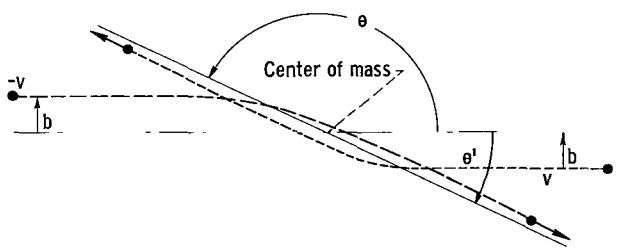

Figure 5. - Scattering of identical particles in center-of-mass system.

$$\sigma_e(\epsilon,\theta) = (1 - P_0)\sigma(\epsilon,\theta) \tag{21}$$

The change in angular dependence from θ to $\pi - \theta$ is required in equation (20) since the particle identities as ion and atom reverse during the charge exchange interaction. For example, if charge transfer occurs during 0° elastic scattering, the interaction will be experimentally indistinguishable from 180° elastic scattering. The angle through which the actual particles are scattered will be referred to as the particle scattering angle, and the angle through which the charge is scattered will be called the apparent scattering angle. (When a distinction between apparent and particle scattering angle is required in notation a prime will be used to denote the particle scattering angle.) Hence, in the preceding example the particle scattering angle is 0° and the apparent scattering angle is 180°.

Classical Elastic Scattering by Polarization Potential

The elastic scattering cross section is given classically by

$$\sigma(\epsilon,\theta) = -\frac{b}{\sin\theta}\frac{db}{d\theta} \tag{22}$$

where b is the impact parameter that produces a scattering angle θ in the center-of-mass system (fig. 5). We now wish to determine $b(\theta)$. This requires solving a two-particle scattering problem in the center-of-mass system, where the two particles with masses m_1 and m_2 are separated by a distance r, have a mutual interaction potential $U(r)$, and are moving with relative velocity u. It is well known (ref. 10) that this problem can be reduced to the equivalent problem of the scattering of a single hypothetical particle with initial velocity u and reduced mass $\mu\left(\mu = \frac{m_1 m_2}{m_1 + m_2}\right)$ about a fixed scattering center. The distance between the hypothetical particle and the scattering center in the single-particle problem corresponds to the distance between particles in the two-particle problem.

The conservation of energy and momentum for the one-particle problem may be written as

$$E_T = \frac{1}{2}\mu(\dot{r}^2 + r^2\dot{\varphi}^2) + U(r) = \frac{1}{2}\mu u^2 = \text{const} \tag{23a}$$

and

$$l = \mu r^2\dot{\varphi} = \mu u b = \text{const}$$

respectively, where r and φ are the polar coordinates of the particle with the origin at the scattering center and $\varphi = 0$ at $r = \infty$ prior to the scattering event. The dots denote differentiation with respect to time. These two equations may be combined to give the following differential equation for the motion of the single particle about the scattering center:

$$\frac{dr}{d\varphi} = \frac{r^2}{b}\sqrt{1 - \frac{b^2}{r^2} - \frac{2U(r)}{\epsilon}} \tag{24}$$

Here it was noted that if $m_1 = m_2 = m$, then E_T is $\frac{1}{2}\epsilon$, where ϵ is $\frac{1}{2}mu^2$.

This equation may be integrated from $\varphi = 0$ at $r = \infty$ to the turning point at φ_0, r_0, where r_0 is the closest approach of the particle to the scattering center. At the point of closest approach $dr/d\varphi = 0$; therefore, r_0 is one of the roots of the equation

$$r^2\sqrt{1 - \frac{b^2}{r^2} - \frac{2U(r)}{\epsilon}} = 0 \tag{25}$$

Furthermore, we can rearrange the energy equation

$$E_T = \frac{1}{2}\mu\dot{r}^2 + V'(r) \tag{23b}$$

where the fictitious potential $V'(r)$ is defined as $\frac{1}{2}\epsilon\frac{b^2}{r^2} + U(r)$. Now we

have an equivalent one-dimensional problem in which the turning point can be seen graphically as the point where $\dot{r} = 0$ and $E = V'$.

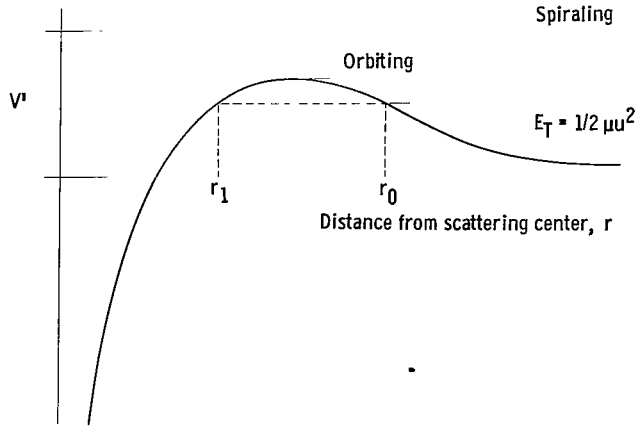

Figure 6. - Fictitious potential for polarization interaction.

A sketch of the fictitious potential for the polarization interaction (fig. 6) shows that r_0 must be the largest root of equation (25); a smaller root would represent a trapped particle rather than one coming in from infinity. The special cases of $r_0 = r_1$ and $r_0 = 0$ being the largest real roots will be discussed later in this section.

When only polarization is considered in the potential function

$$U(r) = -\frac{V}{r^4} \tag{26}$$

where $V = \frac{e^2\alpha}{2}$ (ref. 32), the largest real root of equation (25) is

$$r_0 = 2\sqrt{\frac{\frac{V}{\epsilon b^2}}{1 - \sqrt{1 - \frac{8V}{\epsilon b^4}}}} \tag{27a}$$

and the smaller root (excluding zero) r_1 is

$$r_1 = 2\sqrt{\frac{\frac{V}{\epsilon b^2}}{1 + \sqrt{1 - \frac{8V}{\epsilon b^4}}}} \tag{28}$$

Rearrangement of (27a) gives a relation for the ratio of impact parameter to the distance of closest approach:

$$\frac{b^2}{r_0^2} = 1 + \frac{2V}{\epsilon r_0^4} \tag{27b}$$

By defining

$$y = \frac{r_0}{r} \tag{29}$$

and

$$k = \frac{r_1}{r_0} = \left(\frac{1 - \sqrt{1 - \frac{8V}{\epsilon b^4}}}{1 + \sqrt{1 - \frac{8V}{\epsilon b^4}}} \right)^{1/2} \tag{30}$$

the integral of equation (24),

$$\varphi_0 = \int_{\infty}^{r_0} \frac{b \, dr}{r^2 \sqrt{1 - \frac{b^2}{r^2} - \frac{2U(r)}{\epsilon}}} \tag{31}$$

can be written

$$\theta = 2r_1 b \sqrt{\frac{\epsilon}{2V}} \int_0^1 \frac{dy}{\sqrt{(1 - y^2)(1 - k^2 y^2)}} - \pi \tag{32}$$

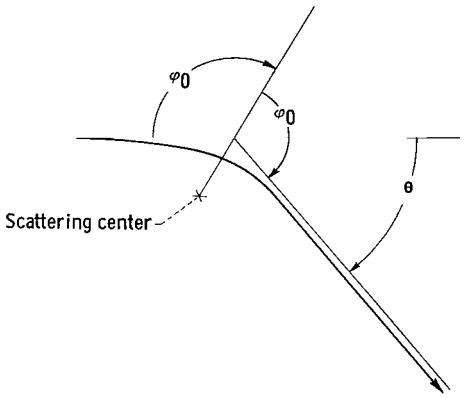

Figure 7. - Relation between scattering angles and angular coordinate.

where the relation between θ and φ_0 obtained from figure 7, $\theta = 2\varphi_0 - \pi$, is used.

The integration in equation (32) can be expressed in terms of a complete elliptic integral of the first kind K(k) by

$$\theta = 2r_1 b \sqrt{\frac{\epsilon}{2V}} K(k) - \pi \tag{33}$$

which can be put into the form

$$\theta = 2 \sqrt{1 + k^2} \, K(k) - \pi \tag{34}$$

by algebraic manipulation of equations (27), (28), (30), and (31). Values of K(k) are tabulated in reference 33.

In order to obtain the cross section, an expression for $db/d\theta$ is required. This is obtained by noting that

$$\frac{db}{d\theta} = \frac{db}{dk} \frac{dk}{d\theta} \tag{35}$$

Performing these differentiations on equations (30) and (34) and inserting them into equation (22) finally yield

$$\sigma(\epsilon,\theta)\sin\theta = \sqrt{\frac{2V}{\epsilon}}\,\frac{1}{4}\,\frac{(1-k^2)^2(1+k^2)^{1/2}}{k^3\left[(1-k^2)K(k)+(1+k^2)B(k)\right]} \tag{36}$$

where the elliptic integral $B(k)$ is also tabulated in reference 33. The angular dependence of the right side of equation (36) is contained in the parameter k via equation (34).

For small scattering angles (less than 0.25 radian) equation (34) may be approximated by

$$\theta \simeq \frac{3\pi}{4}k^2 \tag{37}$$

where terms of the order k^2 and higher have been neglected when compared to unity. To this same approximation, equation (36) becomes

$$\sigma(\epsilon,\theta)\sin\theta \simeq \frac{1}{8\theta^{3/2}}\sqrt{\frac{6\pi V}{\epsilon}} \tag{38}$$

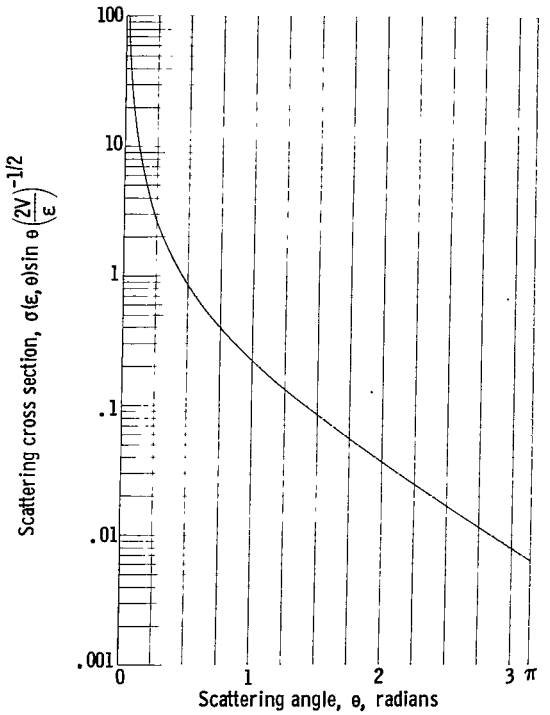

Figure 8. - Classical differential scattering cross section for polarization potential.

The pair of parametric equations (34) and (36) gives the classical differential elastic scattering cross section due to a polarization potential in terms of the parameter k. The angular dependence of the "universal" cross section is presented in figure 8, where the cross section is in units of $\sqrt{2V/\epsilon}$. This separation of angular and energy dependence is characteristic of a classical treatment. The functions $\theta(k)$ and $\left[\frac{\sigma(\epsilon,\theta)\sin\theta}{\sqrt{\frac{2V}{\epsilon}}}\right]_k$ are presented in tables I and II, respectively.

A brief description of the classical particle orbits based on the work in references 13, 14, and 34 follows. The various types of encounters are sketched in figure 9. As the impact parameter decreases below b_π, the incident particle is scattered through more than 180°. Then the interaction cannot be distinguished from one that scattered the incident particle through an angle $-\theta$ nor can it be distinguished from scattering through any angle $2n\pi - \theta$, where n is any integer.

TABLE I. - CLASSICAL SCATTERING ANGLE $\theta(k)$ FOR POLARIZATION POTENTIAL

k^2	0	1	2	3	4	5	6	7	8	9
.0	0	0.2354×10^{-1}	0.4725×10^{-1}	0.7117×10^{-1}	0.9509×10^{-1}	0.1190	0.1432	0.1660	0.1917	0.2160
.1	0.2406	0.2655	0.2903	0.3154	0.3404	0.3658	0.3911	0.4167	0.4425	0.4683
.2	0.4944	0.5208	0.5471	0.5740	0.6009	0.6278	0.6552	0.6826	0.7105	0.7385
.3	0.7667	0.7952	0.8240	0.8531	0.8824	0.9121	0.9420	0.9722	1.0027	1.0335
.4	1.0648	1.0964	1.1283	1.1608	1.1936	1.2269	1.2605	1.2947	1.3293	1.3644
.5	1.4000	1.4360	1.4729	1.5103	1.5481	1.5867	1.6259	1.6659	1.7066	1.7504
.6	1.7906	1.8336	1.8778	1.9229	1.9689	2.0161	2.0644	2.1139	2.1646	2.2168
.7	2.2704	2.3255	2.3822	2.4408	2.5015	2.5640	2.6288	2.6963	2.7661	2.8392
.8	2.9151	2.9946	3.0782	3.1662	3.2591	3.3572	3.4618	3.5736	3.6938	3.8239
.9	3.9658	4.1218	4.4912	4.4912	4.7163	4.9809	5.3035	5.7175	6.2977	7.2850

TABLE II. - CLASSICAL SCATTERING CROSS SECTION $\left[\sigma(\epsilon,\theta)\sin\theta\left(\sqrt{\frac{2V}{\epsilon}}\right)^{-1/2}\right]_k$ FOR POLARIZATION POTENTIAL

k^2	0	1	2	3	4	5	6	7	8	9
.0	∞	104.65	36.478	19.572	12.528	8.8320	6.6177	5.1714	4.1667	3.4368
.1	2.8870	2.4613	2.1243	1.8519	1.6285	1.4426	1.2862	1.1531	1.0387	0.9398
.2	0.8536	0.7779	0.7111	0.6518	0.5990	0.5517	0.5091	0.4707	0.4358	0.4042
.3	0.3754	0.3491	0.3250	0.3028	0.2824	0.2637	0.2463	0.2302	0.2153	0.2015
.4	0.1886	0.1767	0.1655	0.1551	0.1453	0.1362	0.1277	0.1197	0.1122	0.1051
.5	0.9851×10^{-1}	0.9229×10^{-1}	0.8644×10^{-1}	0.8093×10^{-1}	0.7575×10^{-1}	0.7087×10^{-1}	0.6627×10^{-1}	0.6193×10^{-1}	0.5783×10^{-1}	0.5397×10^{-1}
.6	0.5033×10^{-1}	0.4690×10^{-1}	0.4366×10^{-1}	0.4061×10^{-1}	0.3772×10^{-1}	0.3500×10^{-1}	0.3243×10^{-1}	0.3002×10^{-1}	0.2773×10^{-1}	0.2559×10^{-1}
.7	0.2356×10^{-1}	0.2165×10^{-1}	0.1986×10^{-1}	0.1818×10^{-1}	0.1659×10^{-1}	0.1510×10^{-1}	0.1371×10^{-1}	0.1240×10^{-1}	0.1119×10^{-1}	0.1005×10^{-1}
.8	0.8983×10^{-2}	0.7996×10^{-2}	0.7078×10^{-2}	0.6229×10^{-2}	0.5444×10^{-2}	0.4723×10^{-2}	0.4062×10^{-2}	0.3459×10^{-2}	0.2911×10^{-2}	0.2416×10^{-2}
.9	0.1973×10^{-2}	0.1579×10^{-2}	0.1233×10^{-2}	0.9335×10^{-3}	0.6781×10^{-3}	0.4658×10^{-3}	0.2949×10^{-3}	0.1641×10^{-3}	0.7217×10^{-4}	0.1786×10^{-4}

The value of the impact parameter b_π is obtained by rearranging equation (30) to obtain

$$b^2 = \sqrt{\frac{2V}{\epsilon}}\left(\frac{k^2+1}{k}\right) \tag{39}$$

and inserting the solution k_π to the transcendental equation

$$\sqrt{1+k_\pi^2}\,K(k_\pi) = \pi \tag{40}$$

Numerical solution yields $k_\pi = 0.9096$. Then

$$b_\pi^2 = 2\sqrt{\frac{2V}{\epsilon}}\,1.0046 \tag{41}$$

If b is decreased below b_π and the condition $8V/\epsilon b^4 = 1$ is approached, the incident particle begins to orbit the scattering center. This can be seen on examination of equation (30). If $8V/b^4\epsilon = 1$, then $k = 1$, and since $K(1)$ becomes infinite, θ also becomes infinite. Furthermore, we see from equations (27) and (28) that $r_0 = r_1$ when $8V/b^4\epsilon = 1$. This condition is shown in the sketch of fictitious potential (fig. 6).

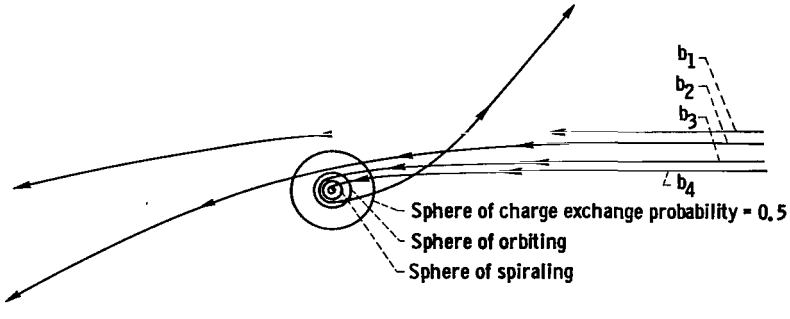

$b_1 > b_2 > b_\pi > b_3 > b_s > b_4$

Figure 9. - Types of encounters in polarization interaction.

For still smaller b corresponding to $8V/b^4\epsilon > 1$, it can be seen from equations (27) and (28) that r_0 and r_1 become imaginary; hence, the largest real root of equation (25) is zero (see fig. 6). Now the incident particle spirals toward the scattering center until short range repulsive potentials control the interaction.[6] The definition of spiraling cross section σ_s is then

$$\sigma_s = \pi b_s^2 \tag{42}$$

where

$$\frac{8V}{\epsilon b_s^4} = 1 \tag{43}$$

The cross section for multiple circuits of the scattering center during scattering $\sigma(\theta > \pi)$ is then given by the annular area between impact parameters b_π and b_s:

$$\sigma(\theta > \pi) = \pi\left(b_\pi^2 - b_s^2\right) \simeq \sigma_s(1.0046 - 1) = 0.0046\ \sigma_s \tag{44}$$

Charge Exchange and Elastic Scattering Differential Cross Sections

The results of the sections RESONANCE CHARGE EXCHANGE PROBABILITY and SEMICLASSICAL DIFFERENTIAL SCATTERING CROSS SECTION can now be combined in the manner indicated by

$$\sigma_x(\epsilon,\theta) = P_0\sigma(\epsilon,\pi - \theta) \tag{20}$$

and

$$\sigma_e(\epsilon,\theta) = (1 - P_0)\sigma(\epsilon,\theta) \tag{21}$$

to obtain the differential charge exchange cross section $\sigma_x(\epsilon,\theta)$ and the differential elastic scattering cross section, respectively. In the section RESONANCE CHARGE EXCHANGE PROBABILITY, it was shown that

$$\begin{aligned} P_0 &= \frac{1}{2} \qquad r < r_{0,c} \\ P_0 &= 0 \qquad r > r_{0,c} \end{aligned} \tag{19}$$

Following the methods of references 25 and 27, the effect of the collision orbit curvature due to polarization on the charge exchange probability may be be ignored, except through its reduction in the distance of closest approach

[6]Spiraling may also be considered as a mechanism by which an ion and an atom are brought sufficiently close together for there to be a high probability of diatomic molecular ion formation (ref. 35).

for a given impact parameter. By using equation (27b) to account for this reduction, equation (19) becomes

$$P_0 = \frac{1}{2} \qquad b \le r_{0,c}\left(1 + \frac{2V}{\epsilon r_{0,c}^4}\right)^{1/2} = b_c$$

$$P_0 = 0 \qquad b > r_{0,c}\left(1 + \frac{2V}{\epsilon r_{0,c}^4}\right)^{1/2} = b_c \tag{45}$$

where $r_{0,c}$ is given by equation (18). The dependence of $\sigma(\epsilon,\theta)$ on scattering angle is available from the parametric equations (34) and (36). For a given scattering angle the corresponding impact parameter is obtained from equations (34) and (39): P_0 is available from equation (45) for this impact parameter. Therefore, for a given scattering angle, both $\sigma(\epsilon,\theta)$ and P_0 can be determined and inserted in equations (20) and (21).

The differential charge exchange cross section and the differential elas-

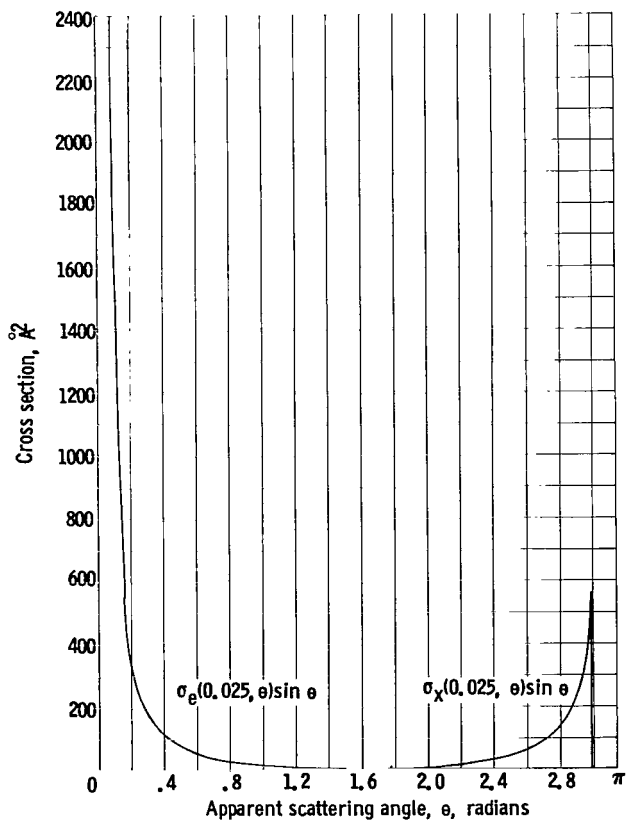

Figure 10. - Differential elastic scattering cross section and differential charge exchange cross section for cesium ions in cesium vapor. Relative energy of collision, 0.025 electron volt.

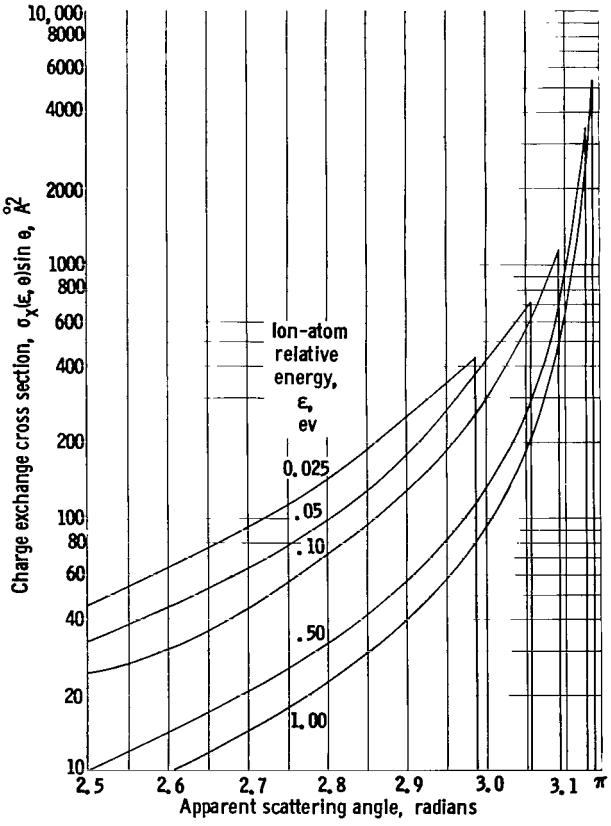

Figure 11. - Differential charge exchange cross section for cesium ions in cesium vapor.

tic scattering cross section were calculated following this procedure and are presented in figure 10 for a cesium ion-atom relative energy of 0.025 electron volt. The following constants were used: A = 27.2 Å, B = 1.53 Å (ref. 19) and α = 52.3 Å^3 (ref. 36). The differential charge exchange cross section is shown in figure 11 for relative energies of 0.025, 0.05, 0.10, 0.50 and 1.00 electron volt. The scale of figure 11 is chosen to illustrate the effect of collision energy on the magnitude of the cross section maximums and cutoff angle θ_c (apparent scattering angle).

An approximate expression indicating the energy dependence of $\sigma_x(\epsilon,\theta_c)$, the maximum value of the differential charge exchange cross section, can be obtained if we note that θ_c', the particle scattering angle, near the maximum is small.

Combining equations (30) and (37), we have

$$\theta_c' = \frac{3\pi}{4}\left(\frac{1 - \sqrt{1 - \frac{8V}{\epsilon b_c^4}}}{1 + \sqrt{1 - \frac{8V}{\epsilon b_c^4}}}\right) \simeq \frac{3\pi}{4}\,\frac{\frac{2V}{\epsilon b_c^4}}{1 - \frac{2V}{\epsilon b_c^4}} \simeq \frac{3\pi}{2}\,\frac{V}{\epsilon b_c^4} \tag{46}$$

where terms of the order of $2V/\epsilon b_c^4$ and smaller have been neglected when compared to unity. Writing equation (27b) to the same degree of approximation gives

$$b_c^2 \simeq r_c^2 \tag{47}$$

so that, by combining equation (18) with the approximate expressions (46) and (47), we obtain

$$\theta_c' = \frac{3\pi^3 V}{8\epsilon(A - B \ln \epsilon)^4} \tag{48a}$$

or

$$\theta_c = \pi - \theta_c' = \pi\left[1 - \frac{3\pi^2 V}{8\epsilon(A - B \ln \epsilon)^4}\right] \tag{48b}$$

This is the particle scattering angle corresponding to the largest impact parameter b_c for which charge exchange can occur. Substituting equation (48) into the small θ approximation of $\sigma(\epsilon,\theta)$, equation (38), and using the result in equation (20) give

$$\sigma_x(\epsilon,\theta_c)\sin\theta_c \simeq \frac{2}{3\pi^4}\,\frac{\epsilon}{V}\,(A - B \ln \epsilon)^6 \tag{49}$$

without making any further approximations.

TOTAL SCATTERING CROSS SECTION

The total scattering cross section with charge exchange due to a polarization potential could be obtained by determining the area under a curve of the type shown in figure 10. Since the differential scattering cross section increases without limit as θ approaches zero the area must be determined as a function of θ_m, an arbitrarily chosen lower limit to the scattering angle. In practice, θ_m is determined by the minimum detectable scattering angle in a scattering chamber apparatus. The total scattering cross section observed in this apparatus would be

$$\sigma_T(\epsilon,\theta_m) = 2\pi \int_{\theta_m}^{\pi} \sigma_e(\epsilon,\theta)\sin\theta\, d\theta + 2\pi \int_{\theta_m}^{\pi-\theta_c'} \sigma_x(\epsilon,\theta)\sin\theta\, d\theta \qquad (50)$$

and if we require $\theta_m < \theta_c'$

$$\sigma_T(\epsilon,\theta_m) = 2\pi \int_{\theta_m}^{\pi} \sigma(\epsilon,\theta)\sin\theta\, d\theta \simeq 2\pi \int_{0}^{b_m} b\, db = \pi b_m^2 \qquad (51)$$

Using equation (39) gives

$$\sigma_T(\epsilon,\theta_m) \simeq \pi \sqrt{\frac{2V}{\epsilon}} \left(\frac{k_m^2 + 1}{k_m} \right) \qquad (52)$$

Since θ_m is always small, equation (34) again may be approximated by equation (37). Combining equations (37) and (52) gives

$$\sigma_T(\epsilon,\theta_m) \simeq \sqrt{\frac{3\pi V}{2\epsilon\theta_m}} \qquad (53)$$

It must be remembered that θ_m is in the center-of-mass system but corresponds to the minimum detectable angle θ_m^L in the laboratory system. The conversion from the center-of-mass system to the laboratory system is given by (ref. 10)

$$\theta_m^L = \frac{\theta_m}{2} \qquad (54)$$

for particles of identical mass.

DIFFUSION CROSS SECTION

The quantity most often needed for charge transport calculations is the diffusion cross section $\sigma_d(\epsilon)$, sometimes called the momentum transfer cross section, which is defined by

$$\sigma_d(\epsilon) = 2\pi \int_0^{\pi} \sigma_e(\epsilon,\theta)(1 - \cos\theta)\sin\theta \, d\theta$$

$$+ 2\pi \int_0^{\pi} \sigma_x(\epsilon,\theta)(1 - \cos\theta)\sin\theta \, d\theta \qquad (55)$$

Noting that $1 - P_0 = 1/2$ for $\theta' \leq \theta \leq \pi$, the first integral in equation (55) becomes

$$2\pi \int_0^{\pi} \sigma_e(\epsilon,\theta)(1 - \cos\theta)\sin\theta \, d\theta = 2\pi \int_0^{\theta_c'} \sigma(\epsilon,\theta)(1 - \cos\theta)\sin\theta \, d\theta$$

$$+ 2\pi \int_{\theta_c'}^{\pi} \frac{1}{2} \sigma(\epsilon,\theta)(1 - \cos\theta)\sin\theta \, d\theta \qquad (56)$$

The second integral in equation (55) can likewise be written

$$2\pi \int_0^{\pi} \sigma_x(\epsilon,\theta)(1 - \cos\theta)\sin\theta \, d\theta = \pi \int_{\theta_c'}^{\pi} \sigma(\epsilon,\theta)(1 + \cos\theta)\sin\theta \, d\theta \qquad (57)$$

Adding equations (56) and (57) now gives

$$\sigma_d(\epsilon) = 2\pi \int_{\theta_c'}^{\pi} \sigma(\epsilon,\theta)\sin\theta \, d\theta + 2\pi \int_0^{\theta_c'} \sigma(\epsilon,\theta)(1 - \cos\theta)\sin\theta \, d\theta \qquad (58)$$

The first integral on the right is just $\sigma_T(\epsilon,\theta_c')$ given by equation (53). Using the small angle approximation for $\sigma(\epsilon,\theta)$ given by equation (38) and the further small angle approximation

$$1 - \cos\theta \simeq \frac{\theta^2}{2} \qquad (59)$$

the second term on the right in equation (58) becomes

$$\frac{\pi}{8} \int_0^{\theta_c'} \sqrt{\frac{6\pi V\theta}{\epsilon}} \, d\theta$$

which can be integrated to yield

$$\frac{\pi}{12} \sqrt{\frac{6\pi V}{\epsilon}} \, (\theta_c')^{3/2}$$

Now equation (58) gives

$$\sigma_d(\epsilon) = \pi \sqrt{\frac{3\pi V}{2\epsilon\theta_c'}} + \frac{\pi}{12} \sqrt{\frac{6\pi V}{\epsilon}} (\theta_c')^{3/2} = \sigma_T\left[1 + \frac{1}{6}(\theta_c')^2\right] \tag{60}$$

so the diffusion cross section may be approximated by

$$\sigma_d(\epsilon) \simeq \sigma_T(\epsilon,\theta_c') \tag{61}$$

It is also worth noting that

$$\sigma_x(\epsilon) = 2\pi \int_0^{\pi} \sigma_x(\epsilon,\theta)\sin\theta\, d\theta = \pi \int_{\theta_c'}^{\pi} \sigma(\epsilon,\theta)\sin\theta\, d\theta \tag{62}$$

Comparison with equation (58) gives the well-known expression (ref. 30)

$$\sigma_d(\epsilon) \simeq 2\sigma_x(\epsilon) \tag{63}$$

to the same degree of approximation as equation (61).

SCATTERING CHAMBER EXPERIMENTS

Theory

Consider the passage of an ion beam through a chamber containing its own vapor (fig. 12).

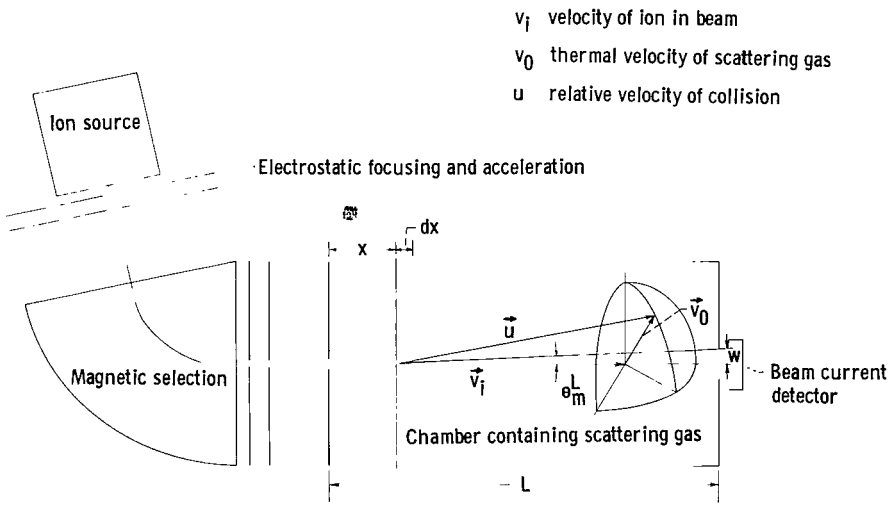

Figure 12. - Typical scattering chamber apparatus.

Let $N_0 = \int_{\vec{v}_0} N_0 f_0(\vec{v}_0) d\vec{v}_0$ = scattering gas density in particles per cubic centimeter, where $f(\vec{v}_0)d\vec{v}_0$ is the normalized velocity distribution function

for the gas. Likewise, let $n_i = \int_{\vec{v}_i} n_i f_i(\vec{v}_i) d\vec{v}_i$ = ion density in particles per cubic centimeter, where $f_i(\vec{v}_i)d\vec{v}_i$ is the normalized ion velocity distribution function for the beam ions.

The rate at which ions are scattered from the beam per unit volume is given by

$$\frac{dn_i(t)}{dt} = -\int_{\vec{v}_0}\int_{\vec{v}_i} N_0 f_0(\vec{v}_0) n_i(t) f_i(\vec{v}_i) u(\vec{v}_0,\vec{v}_i) \sigma_T\left(\epsilon,\theta_m^L\right) d\vec{v}_0\, d\vec{v}_i \tag{64}$$

where $\epsilon = \frac{1}{2} mu^2$ (m is the ion or atom mass), u is the ion-atom relative velocity (fig. 12), and $\sigma_T\left(\epsilon,\theta_m^L\right)$ is the total cross section for scattering through angles greater than θ_m^L in the laboratory system.

If we have a well-collimated monoenergetic ion beam

$$f_i(\vec{v}_i) = \delta(v_i)$$

and

$$\frac{dn_i(t)}{dt} = -\, n_i(t) N_0 \int_{\vec{v}_0} f_0(\vec{v}_0) u(\vec{v}_0, v_i) \sigma_T\left(\epsilon,\theta_m^L\right) d\vec{v}_0 \tag{65}$$

so

$$n_i(T) = n_i(0)\exp\left[-N_0 \int_0^T \int_{\vec{v}_0} f_0(\vec{v}_0) u(\vec{v}_0, v_i) \sigma_T\left(\epsilon,\theta_m^L\right) d\vec{v}_0\, dt\right] \tag{66}$$

where T is the time required for a longitudinal element of the beam to traverse the scattering chamber $T = L/v_i$. Changing the variable of integration from t to x, the length of the scattering chamber traversed by the beam element, and multiplying through by eAv_i to obtain equation (66) in terms of beam current give

$$I(L) = I(0)\exp\left[-\frac{N_0}{v_i}\int_0^L \int_{\vec{v}_0} f_0(\vec{v}_0) u(\vec{v}_0, v_i) \sigma_T\left(\epsilon,\theta_m^L\right) d\vec{v}_0\, dx\right]$$

$$= I(0)e^{-pP_c L} \tag{67}$$

where p is the gas pressure in the scattering chamber, and the collision

probability P_c is defined[7] by

$$P_c \equiv \frac{N_0}{pv_i L} \int_0^L \int_{\vec{v}_0} f_0(\vec{v}_0) u(\vec{v}_0, v_i) \sigma_T \left(\epsilon, \theta_m^L\right) d\vec{v}_0 \, dx \tag{68}$$

This is a generalization of the definition given in reference 3

$$P_c \equiv \frac{N_0}{p} \bar{\sigma} \tag{69}$$

where $\bar{\sigma}$ is the collision cross section.

We now need the geometric relation between θ_m^L and x. From figure 12 we obtain

$$\theta_m^L = \tan^{-1} \frac{w}{L - x} = \frac{w}{L - x} - \frac{1}{3} \left(\frac{w}{L - x}\right)^3 + \cdots \simeq \frac{w}{L - x} \tag{70}$$

In order for this approximation to be valid, it is necessary that

$$1 - \frac{x}{L} \gg \frac{w}{L}$$

Since w/L is of the order of 10^{-3} or 10^{-4} for a typical scattering chamber (ref. 1), the approximate form of equation (70) should be accurate over more than 99.9 percent of the chamber length.

By inserting equations (53), (54), and (70) into (68), we have

$$P_c = \frac{\pi N_0}{pv_i L} \sqrt{\frac{3\pi V}{2m}} \int_0^L \int_{\vec{v}_0} f_0(\vec{v}_0) \sqrt{\frac{L - x}{w}} \, dv_0 \, dx \tag{71}$$

Integrating with respect to gas atom velocity gives

$$P_c = \frac{\pi N_0}{pv_i L} \sqrt{\frac{3\pi V}{2m}} \int_0^L \sqrt{\frac{L - x}{w}} \, dx \tag{72}$$

Now integrating over the distance traversed in the chamber yields

$$P_c = \frac{\pi N_0}{pv_i} \sqrt{\frac{2\pi VL}{3mw}} \tag{73}$$

[7]Maxwell (ref. 37) was the first to point out the lack of dependence of the velocity integration of equation (68) on the normalized velocity distribution function for an inverse fourth power potential; however, Maxwell's potential was inverse fourth repulsion.

Comparison with equation (69) and using $\epsilon = \frac{1}{2} mv_i^2$, which assumes stationary target atoms, give

$$\overline{\sigma} = \pi \sqrt{\frac{\pi V}{3\epsilon} \frac{L}{w}} \tag{74}$$

the total cross section for scattering through angles greater than the angular resolution of the apparatus.

This would be the expected result of an experimental determination of P_c by the usual scattering chamber technique. The collision probability is experimentally determined in the following manner: The ion beam current I_L, which passes through the scattering chamber, is observed for several values of chamber pressure p_0 with constant ion beam current and velocity entering the chamber. A semilogarithmic plot of I_L against p_0 gives a straight line the slope of which is $-P_c L$ (see eq. (67)).

Experiments

Cesium. - The total cross section of cesium ions traveling through their own vapor has been measured for energies between 0.12 and 10.0 electron volts (ref. 38). The experiment is comparable in principle with the sketch in figure 12, the difference being that the collision chamber of reference 38 is curved and placed in a magnetic field. This design defines the ion energy more precisely than purely electrostatic methods. The value of w/L is about 0.00073 or an average angular resolution θ_m^L of about 0.0015 radian (information received in a private communication with R. H. Bullis, R. K. Flavin, and R. G. Meyerand, Jr. of United Aircraft Corp.).

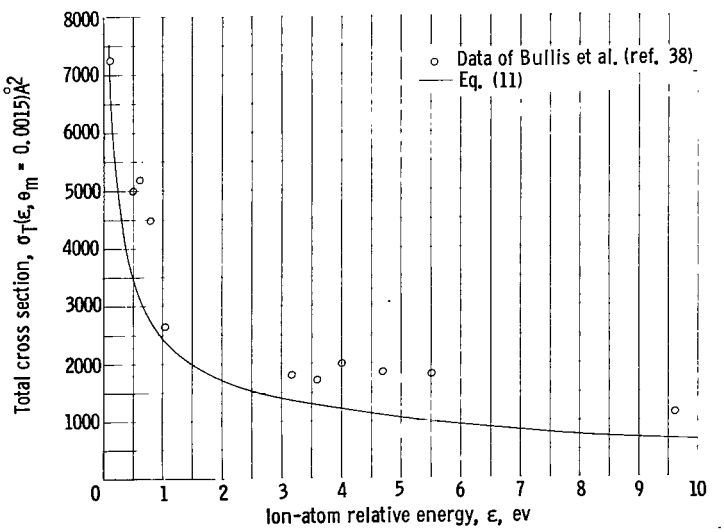

Figure 13. - Total scattering cross section. Comparison of Bullis et al. data (ref. 38) with semiclassical theory for cesium ions in cesium vapor.

The data of reference 38 are shown in figure 13. Equation (74) is plotted in the same figure for $w/L = 0.00073$.

Inert gases. - An apparatus similar to the one presented in figure 12 was designed for investigation of the total collision cross section of inert gas ions in the inert gases (ref. 39). This apparatus had a w/L ratio of about 0.0365, that is, an average angular resolution of about 0.073 radian. Data from references 39 to 41 are presented in figures 14 and 15 for argon ions in argon gas and neon ions in neon gas, respectively.

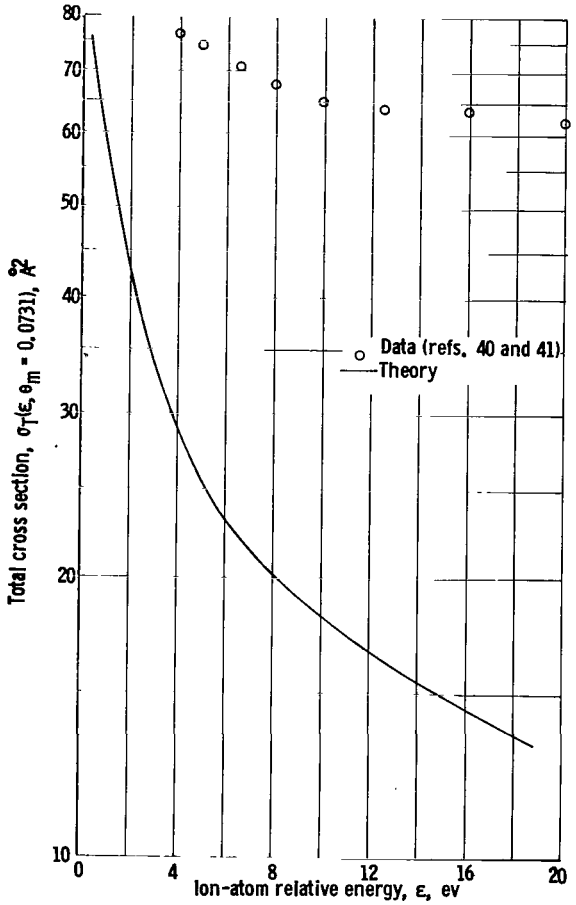

Figure 14. - Total scattering cross section. Comparison of data from references 40 and 41 with semiclassical theory for argon ions in argon gas.

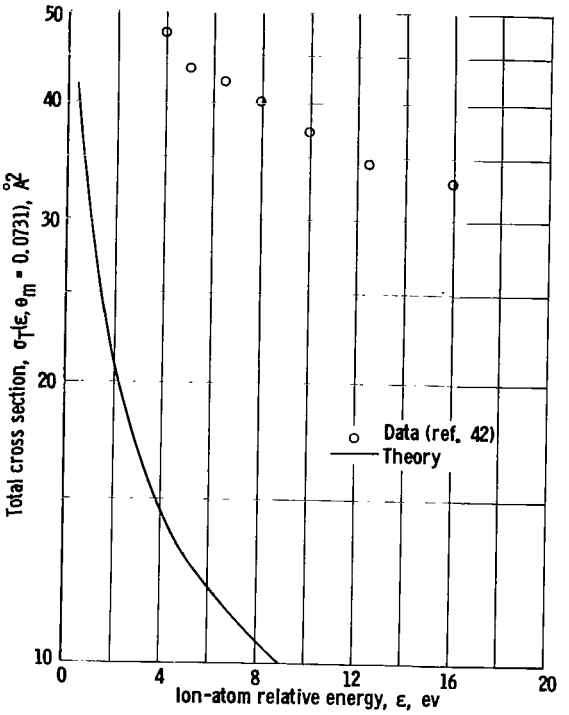

Figure 15. - Total scattering cross section. Comparison of data from reference 42 with semiclassical theory for neon ions in neon gas.

Equation (74) is also shown in these figures for comparison.

DISCUSSION

Limitations of the Theory

The cross section theory presented herein contains inaccuracies due to the semiclassical approach to the scattering problem, the simple choice of interaction potential, and the adiabatic assumption and various mathematical approximations made in computing charge exchange probability.

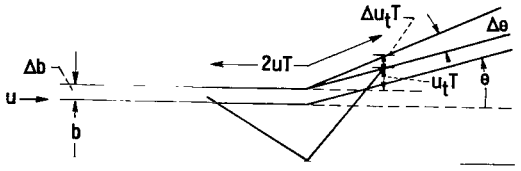

Figure 16. - Uncertainty in impact parameter and scattering angle.

If classical calculations are to be performed for an atomic scattering event, the quantum mechanical limits on the validity of this computation must be considered. These limits are imposed by the uncertainty relation (ref. 15)

$$m \, \Delta u_t \, \Delta b \simeq h \qquad (75)$$

where m is the particle mass, u_t its transverse velocity, and b is again the impact parameter (fig. 16). The symbol Δ indicates uncertainty in the quantity which follows it. In order for a classical treatment to be valid, we must have

$$\theta \gg \Delta\theta = \frac{\Delta u_t}{u}$$

$$b \gg \Delta b$$

Using equation (75) and $\epsilon = \frac{1}{2} mu^2$, we find that the classical treatment fails for scattering angles less than θ^*, where

$$\theta^* \simeq \frac{h}{\sqrt{2m\epsilon}\, b} \tag{76}$$

The true total elastic scattering cross section should actually be smaller than the classically calculated value obtained from equation (53) for scattering angles less than θ^*. The classical value becomes infinite as θ_m approaches zero. It is well known, however, that the quantum mechanical calculation gives finite cross sections as zero scattering angle is approached, if the scattering potential falls off more rapidly than $1/r^2$ (ref. 42). The dependence of θ^* on energy is shown in figure 17 for cesium, where it may be compared with θ_c'. Note that, over a wide range of scattering angle for which classical mechanics fails, the charge exchange probability is zero; that is,

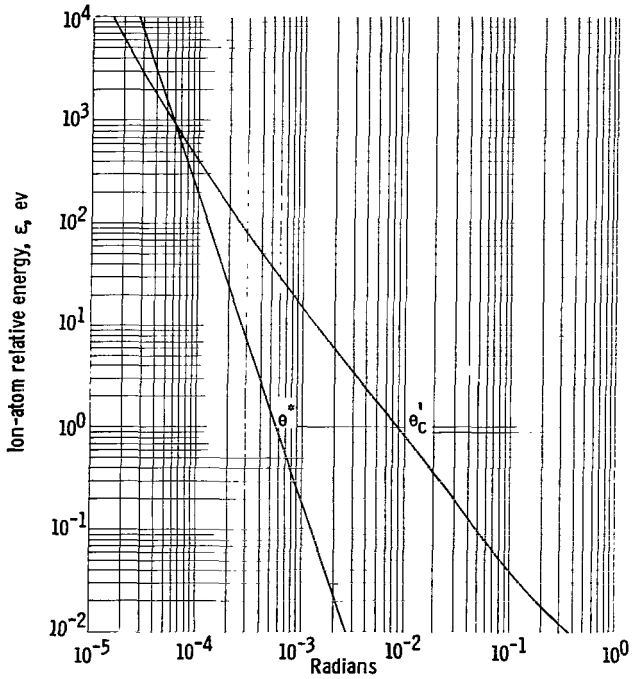

Figure 17. - Critical particle scattering angle θ_c' and lower limit for valid classical calculation θ^* for cesium.

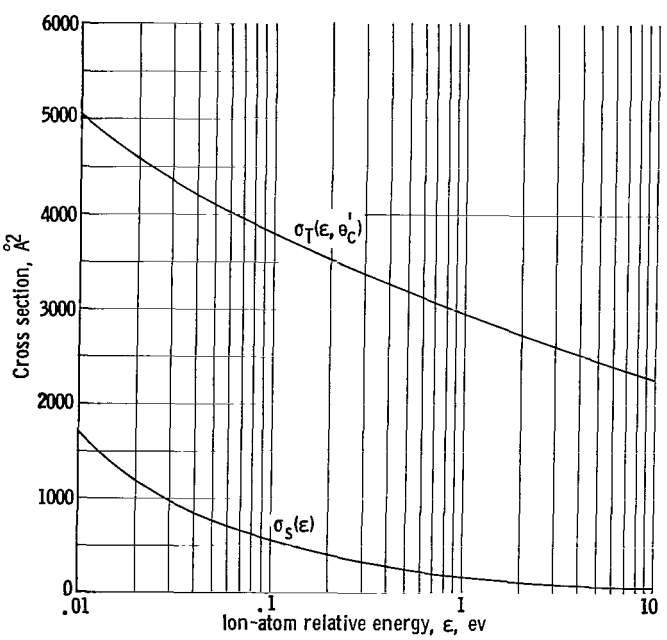

Figure 18. - Comparison of total scattering cross section $\sigma_T(\epsilon, \theta_c')$ with spiraling cross section $\sigma_S(\epsilon)$.

$$\theta_c' > \theta^*$$

Hence, little error should be introduced in figures 10 and 11 (p. 17) by the classical orbit assumption.

At very large elastic scattering angle, which implies close approach of the interacting nuclei, the assumption of pure polarization interaction is a poor one. Under these conditions, orbiting or spiraling may occur, and a more elaborate potential function including repulsive forces must be considered. The main interest, however, is not in large particle scattering angles where, as can be seen in figure 8 (p. 14), the differential scattering cross section is relatively small.

In the case of cesium, only at low thermal energy is the spiraling cross section significant. A comparison of the cesium spiraling cross section obtained from equations (42) and (43) and the total scattering cross section obtained from equations (61) and (63) and an extrapolation of cesium charge exchange cross section data (ref. 19) is made in figure 18. If the collision energy is greater than 0.025 electron volt, the spiraling cross section is less than 25 percent of the total scattering cross section. This percentage decreases with increasing energy.

The use of equation (19) to obtain the charge exchange probability is an approximation to the more accurate form of the probability sketched in figure 4 (p. 9). This simplification was made following the method of reference 25. The use of the exponential tail instead of chopping the probability at b_c would be expected to round the cutoff peak slightly at θ_c and smooth the discontinuity in $\sigma_e(\epsilon,\theta)$ at θ_c'.

The calculation of charge exchange probability required the use of the approximate expressions

$$e^{i\frac{m_e u x}{\hbar}} \simeq 1 \tag{12}$$

and

$$e^{-\frac{i}{\hbar}\frac{m_e u^2}{2}t} \simeq 1 \tag{13}$$

These expressions were shown, in the discussion of resonance charge exchange probability, to be equivalent to the condition

$$\frac{m_e u D}{\hbar} \ll 1$$

The physical meaning of this condition is clear if we consider the angular momentum relation for an electron orbiting with velocity v_e in a Bohr orbit of radius r_e

$$m_e v_e r_e = n\hbar \tag{77}$$

where n is the principal quantum number. If we consider a hydrogen-like atom in the ground state $n = 1$ and if the range of the interaction D is of the order of atomic dimensions so that $D/r_e \simeq 1$, we see that

$$\frac{m_e u D}{\hbar} = \frac{u}{v_e}\frac{D}{r_e} \simeq \frac{u}{v_e}$$

so the condition for the approximate equations (12) and (13) to hold is

$$\frac{u}{v_e} \ll 1$$

that is, the relative velocity of the colliding nuclei must be much less than the velocity of the orbiting electron that is to be exchanged. This is the so-called adiabatic approximation. Since for the first Bohr orbit

$$v_e = \frac{e^2}{\hbar^2} = 3.5\times10^7 \text{ cm/sec}$$

the adiabatic condition for a cesium ion-atom collision requires that the relative kinetic energy be less than 85 kiloelectronvolt.

We see from the previous discussion that the validity of this analysis is dependent on the following three conditions:

(1) $\theta^* < \theta_m < \theta_c'$

(2) $\sigma_s \ll \sigma_T$

(3) $u/v_e \ll 1$

Condition (1) presupposes $\theta^* < \theta_c'$, which is not necessarily true at high energy. This condition rather than condition (3) often establishes the upper limit on the energy range. Cesium, which is used as an example of interest, is limited not by the 85 kiloelectronvolt adiabatic limitation of condition (3), but by condition (1) (see fig. 17), where $\theta^* = \theta_c'$ for a collision energy of about 1000 electron volts.

Comparison of Theory with Experiment

There is only a limited quantity of data in the open literature that meets the three conditions discussed, and these data are only in the form of total cross section measurements; there are no data on differential scattering cross sections of low energy ions in their own gas. It would seem that cesium is the only element whose unique combination of properties (large mass, large polarizability, and interesting applications requiring low energy collisions) make it

suitable for application of the theory at energies between 0.025 and 1000 electron volts.

The observations of total cesium scattering cross sections made by Bullis, et al. (ref. 38) have been compared with the theory in figure 13. While the agreement might be termed acceptable, it must be admitted that the data do tend to fall above the theoretical curve. This is particularly true in the low energy range, that is, below 1 electron volt. The experimenters have, however, been quick to point out (information received in a private communication with R. H. Bullis, R. K. Flavin, and R. G. Meyerand, Jr. of United Aircraft Corp.) the difficulties of making measurements in this low energy range and that these are only preliminary data. Their low energy ion beam tends to space-charge spread or be deflected by stray electric fields arising from charges on insulators and field penetration of the scattering chamber. The low intensity ion beam signal requires a nude electron multiplier type detector whose gain tends to drift in the low pressure cesium environment. Any of these effects could give an erroneously high value of cross section. A noteworthy attempt to overcome these difficulties was made by fabricating the entire collision chamber including the end slits from a single piece of electrolytically deposited copper. Furthermore, the end slits were contoured to minimize field penetration. Extensive cold trapping and pumping were used to reduce the background cesium pressure in the region of the electron multiplier. Still one must remember, when comparing the experimental data with theory, that there exists the possibility of a systematic error that gives high values of cross section.

It is also interesting to compare the total scattering cross section predicted by equation (74) with the observations from reference 40 for argon ions and from reference 41 for neon ions in their parent gases (figs. 14 and 15, respectively). The theory is not applicable to these data, since $\theta_m \simeq 0.073$ for the apparatus of reference 39 and $\theta_c' < 0.02$ for collision energies greater than 1.0 electron volt for both neon and argon. It is also to be expected that the theory would not explain inert gas interactions, since hydrogen-like wave functions were used to obtain the theoretical charge exchange probability.

The approach of the experimental results to the theory at low energy is noteworthy. The true cross section is expected to be larger than the prediction of equation (74) when $\theta_m > \theta_c'$, because any charge exchange interaction that results in particle scattering angles between θ_m and θ_c' has not been included in the calculation. From this standpoint, the data in figures 12, 14, and 15 are in fair agreement with the theory.

CONCLUSIONS

The semiclassical calculation of differential charge exchange cross section is only an approximate method; however, several interesting features of the results are expected to be valid. These features would be exhibited not only for the cesium resonance interaction, for which numerical values have been given, but for any resonance charge exchange interaction that satisfies the three conditions:

(1) $\theta^* < \theta_m < \theta_c'$

(2) $\sigma_s \ll \sigma_T$

(3) $u < v_e$

These conditions can be satisfied for cesium if the ion-atom relative energy of collision is between 0.025 and 1000 electron volts.

As the calculations for cesium have shown, the differential charge exchange cross section has a cutoff close to, but not at, an apparent scattering angle of 180°. The maximum value of the cross section occurs at the cutoff angle. As the collision energy increases, the cutoff angle approaches 180° and the cross section maximum increases. The values of the cutoff angle and cross section maximum may be approximated by the expressions

$$\theta_c \simeq \pi\left[1 - \frac{3\pi^2 V}{8\epsilon(A - B \ln \epsilon)^4}\right] \tag{48b}$$

and

$$\sigma_x(\epsilon,\theta_c) \simeq \frac{2}{3\pi^4}\frac{\epsilon}{V}(A - B \ln \epsilon)^6 \tag{49}$$

respectively.

The total cross section for scattering through angles greater than θ_m was found by integration to be approximately given by

$$\sigma_T(\epsilon,\theta_m) \simeq \pi\sqrt{\frac{3\pi V}{2\epsilon\theta_m}} \tag{53}$$

subject to the condition $\theta_m < \theta_c'$ and the corresponding collision probability expected as the result of a scattering chamber type experiment is

$$P_c = \frac{\pi N_0}{pv_i}\sqrt{\frac{2\pi VL}{3mw}} \tag{73}$$

The expressions

$$\sigma_d(\epsilon) \simeq \sigma_T(\epsilon,\theta_c')$$

and

$$\sigma_d(\epsilon) \simeq 2\sigma_x(\epsilon) \tag{63}$$

have been shown to be valid even though the differential cross section vanishes at an apparent scattering angle of 180°.

Lewis Research Center
National Aeronautics and Space Administration
Cleveland, Ohio, June 24, 1964

APPENDIX - INTEGRATION OF CHARGE EXCHANGE PROBABILITY EXPRESSION FOR HYDROGEN-LIKE ATOMS

It was indicated in the main text that the charge exchange probability may be given by

$$P_0 = \left| \frac{i}{\hbar} \int_{-\infty}^{\infty} \left[\int_{\text{all space}} \varphi_0(r) U_A(r') \psi_0(r') d\tau \right] dt \right|^2 \tag{A1}$$

where

$$\varphi_0 = \sqrt{\frac{z^3}{\pi a^3}}\, e^{-\frac{z}{a} r} \tag{A2}$$

$$\psi_0(r') = \sqrt{\frac{z^3}{\pi a^3}}\, e^{-\frac{z}{a} r'} \tag{A3}$$

$$U_a(r') = -\frac{e^2}{r'} \tag{A4}$$

The integral over spatial coordinates is then

$$I = -\int_{\text{all space}} \frac{z^3}{\pi a^3} e^{-\frac{z}{a}(r+r')} \left(\frac{e^2}{r'}\right) d\tau \tag{A5}$$

Referring to the coordinate system in figure 3 with χ taken as the angle between $\vec{R}$ and $\vec{r}$ shows that

$$\vec{r} - \vec{R} = \vec{r}'$$

and

$$r' = \sqrt{R^2 + r^2 - 2rR \cos \chi}$$

Then equation (A5) becomes

$$I = -\left(\frac{z^3 e^2}{\pi a^3}\right) \int_0^{\infty} 2\pi r^2 e^{-\frac{z}{a} r} \left(\int_0^{\pi} \frac{e^{-\frac{z}{a}\sqrt{R^2+r^2-2rR\cos\chi}}}{\sqrt{R^2 + r^2 - 2rR \cos \chi}} \sin \chi \, d\chi \right) dr \tag{A6}$$

Performing the integration over χ yields

$$I = \left(\frac{z^3e^2}{\pi a^3}\right)\frac{2\pi a}{zR}\int_0^\infty re^{-\frac{z}{a}r}\left[e^{-(R+r)\frac{z}{a}} - e^{-\frac{z}{a}|r-R|}\right]dr$$

which can be written as

$$I = \left(\frac{2z^2e^2}{a^2R}\right)\left(e^{-\frac{Rz}{a}}\int_0^\infty re^{-\frac{2zr}{a}}\,dr - e^{-\frac{Rz}{a}}\int_0^R r\,dr - e^{\frac{Rz}{a}}\int_R^\infty re^{-\frac{2zr}{a}}\,dr\right)$$

Now integrating over r gives

$$I = \left(-\frac{z^2e^2}{a}\right)\left(1 + \frac{zR}{a}\right)e^{-\frac{Rz}{a}} \tag{A7}$$

The charge exchange probability, equation (A1), is now

$$P_0 = \left|\frac{z^2e^2}{a\hbar}\int_{-\infty}^\infty \left[1 + \frac{zR(t)}{a}\right]e^{-\frac{R(t)z}{a}}\,dt\right|^2 \tag{A8}$$

Referring to figure 3, we see that

$$R(t) = \sqrt{R_0^2 + u^2t^2}$$

So we now need the integral

$$J = \int_{-\infty}^\infty \left(1 + \frac{z}{a}\sqrt{R_0^2 + u^2t^2}\right)e^{-\frac{z}{a}\sqrt{R_0^2+u^2t^2}}\,dt \tag{A9}$$

By noting the symmetry of the integrand, equation (A9) can be written

$$J = 2\int_0^\infty \left(1 + \frac{z}{a}\sqrt{R_0^2 + u^2t^2}\right)e^{-\frac{z}{a}\sqrt{R_0^2+u^2t^2}}\,dt$$

Making the substitution

$$x^2 = R_0^2 + u^2t^2$$

gives

$$J = \frac{2}{u} \int_{R_0}^{\infty} \left(1 + \frac{z}{a} x\right) e^{-\frac{z}{a} x} \frac{x \, dx}{\sqrt{x^2 - R_0^2}}$$

Integrating by parts and making the substitutions $\xi = x/R_0$ and $\rho = R_0 z/a$, we obtain

$$J = \frac{2}{u} \left(\frac{z}{a}\right)^2 R_0^3 \int_1^{\infty} \xi(\xi^2 - 1)^{1/2} e^{-\rho\xi} \, d\xi \tag{A10}$$

From reference 44 we obtain

$$K_n(\rho) = \frac{\Gamma\left(\frac{1}{2}\right)}{\Gamma\left(n + \frac{1}{2}\right)} \left(\frac{\rho}{2}\right)^n \int_1^{\infty} e^{-\rho\xi} (\xi^2 - 1)^{n-1/2} \, d\xi \tag{A11}$$

where $K_n(\rho)$ is the modified Bessel function of the second kind. Differentiating equation (A11) with respect to ρ and using

$$\frac{dK_n(\rho)}{d\rho} = -K_{n-1}(\rho) - \frac{n}{\rho} K_n(\rho)$$

give

$$\int_1^{\infty} \xi(\xi^2 - 1)^{n-1/2} e^{-\rho\xi} \, d\xi = \frac{\Gamma\left(n + \frac{1}{2}\right)}{\Gamma\left(\frac{1}{2}\right)} \left(\frac{2}{\rho}\right)^n \left[K_{n-1}(\rho) + 2 \frac{n}{\rho} K_n(\rho)\right] \tag{A12}$$

which, for $n = 1$, yields

$$\int_1^{\infty} \xi(\xi^2 - 1)^{1/2} e^{-\rho\xi} \, d\xi = \frac{1}{\rho} \left[K_0(\rho) + \frac{2}{\rho} K_1(\rho)\right] \tag{A13}$$

Substituting equation (A13) into equation (A10) gives

$$J = \frac{2R_0}{u} \rho\left[K_0(\rho) + \frac{2}{\rho} K_1(\rho)\right] \tag{A14}$$

Now the charge exchange probability, equation (A8), becomes

$$P_0 = \left| \frac{2ze^2}{\hbar u} \rho\left[\rho K_0(\rho) + 2K_1(\rho)\right] \right|^2 \tag{A15}$$

For large ρ we may use the approximate expressions (ref. 33)

$$K_0(\rho) \simeq K_1(\rho) \simeq \sqrt{\frac{\pi}{2\rho}}\, e^{-\rho} \tag{A16}$$

so that to this degree of approximation, equation (A15) may be written as

$$P_0 = \left(\frac{e^2}{\hbar u}\right)^2 2\pi z^2 \rho(\rho + 2)^2 e^{-2\rho} \tag{A17}$$

REFERENCES

1. Massey, H. S. W., and Burhop, E. H. S.: Electronic and Ionic Impact Phenomena. Clarendon Press (Oxford), 1952.

2. Massey, H. S. W.: Collisions Between Atoms and Molecules at Ordinary Temperatures. Rep. on Prog. in Phys., 1949, pp. 248-269.

3. Brown, Sandborn Conner: Basic Data of Plasma Physics. Cambridge Tech. Press, M.I.T., 1959.

4. Nottingham, Wayne B.: General Theory of the Plasma Diode Energy Converter. Tech. Rep. TEE 7002-5, Thermo Electron Eng. Corp., 1960.

5. Nottingham, W. B.: Production of Cesium Ions in a Strong Ion Accelerating Field. Paper Presented at Annual Conf. on Phys. Electronics, M.I.T., Mar. 1963.

6. Kaplan, C.: Investigation of the Current Density Limitations in a Thermionic Converter. Rep. 25,081, The Marquardt Corp., 1963.

7. Kerslake, William R.: Charge-Exchange Effects on the Accelerator Impingement of an Electron-Bombardment Ion Rocket. NASA TN D-1657, 1963.

8. Muschlitz, E. E., Jr., and Simons, J. H.: The Measurement of Electron Exchange in Gases at Low Pressure. Jour. Phys. Chem., vol. 56, no. 7, Oct. 20, 1956, pp. 837-841.

9. Mason, Edward A., and Vanderslice, Joseph T.: Elastic Scattering of Slow Ions in Gases. Jour. Chem. Phys., vol. 31, no. 3, Sept. 1959, pp. 594-600.

10. Goldstein, H.: Classical Mechanics. Addison-Wesley Pub. Co., Inc., 1950.

11. Mason, Edward A., and Schamp, Homer W., Jr.: Mobility of Gaseous Ions in Weak Electric Fields. Ann. Phys., vol. 4, 1958, pp. 233-270.

12. Hirschfelder, Joseph O., Curtiss, Charles F., and Bird, R. Byron: Molecular Theory of Gases and Liquids, John Wiley & Sons, Inc., 1954.

13. McDaniel, E. W.: Langevin's Theory of the Mobility of Gaseous Ions. Tech. Rep. 4, Eng. Experiment Station, Georgia Inst. Tech., Aug. 1, 1960.

14. MacMillan, W. D.: The Motion of a Particle Attracted Towards a Fixed Center by a Force Varying Inversely as the Fifth Power of the Distance. Am. Jour. Math., vol. 5, 1907, pp. 282-306.

15. Bates, D. R.: Atomic and Molecular Impact Phenomena. Academic Press, 1962.

16. Sena, L. A.: Stolknoveniya Elektronov i Ionov s Atomami Gaza (Collisions of Electrons and Ions with Gas Atoms). Moscow-Leningrad: Gostekhizdat, 1948.

17. Heinz, O., and Feinler, E. J.: Tabulation of Atomic and Molecular-Charge Transfer Cross Sections. Interim Tech. Rep. 1, Stanford Res. Inst., Jan. 20, 1961.

18. Speiser, R. C.: Cesium Ion-Atom Charge Exchange Scattering. Rep. 1583, Electro-Optical Systems, Inc., Sept. 30, 1961.

19. Marino, Lawrence L., Smith, A. C. H., and Caplinger, E.: Charge Transfer Between Positive Cesium Ions and Cesium Atoms. Phys. Rev., vol. 128, no. 5, Dec. 1962, pp. 2243-2250.

20. Kushnir, R. M., and Buchma, I. M.: Further Investigation of Resonance Charge Exchange of Positive Cesium Ions. Bull. Acad. Sci. USSR, Phys. Ser., vol. 24, no. 7, 1960, pp. 989-992.

21. Bukhteev, A. M., and Bydin, Yu. F.: Resonance Charge Exchange of Alkali Metal Ions and Atoms. Bull. Acad. Sci. USSR, Phys. Ser., vol. 24, nos. 7-12, 1960, pp. 966-971.

22. Chkuaseli, D. V., Nikoleishvili, U. D., and Guldamashvili, A. I.: Resonance Charge Exchange of Positive Alkali Metal Ions. Bull. Acad. Sci. USSR, Phys. Ser., vol. 24, nos. 7-12, 1960, pp. 972-976.

23. Kushnir, R. M., Palyukh, B. M., and Sena, L. A.: Investigation of Resonance Charge Exchange in Monatomic Gases and Metal Vapors. Bull. Acad. Sci. USSR, Phys. Ser., vol. 23, nos. 7-12, 1959, pp. 995-999.

24. Firsov, O. B.: Resonance-Exchange of Ions in Slow Collisions. Zh. Eksper. Teor. Fiz., vol. 21, no. 9, 1951, pp. 1001-1008.

25. Holstein, T.: Mobilities of Positive Ions in Their Parent Gases. Jour. Phys. Chem., vol. 56, no. 7, Oct. 20, 1952, pp. 832-836.

26. Mott, N. F.: Theory of Excitation by Collision with Heavy Particles. Proc. Cambridge Phil. Soc., vol. 27, Oct. 31, 1931, pp. 553-560.

27. Demkov, Yu. N.: Quantum Mechanical Calculation of Charge Exchange Probability During Collisions. Annales Leningrad Univ., vol. 146, 1952, p. 74.

28. Massey, H. S. W., and Smith, R. A.: The Passage of Positive Ions Through Gases. Proc. Roy. Soc. (London), ser. A, vol. 142, Nov. 1933, pp. 142-172.

29. Bates, D. R., Massey, H. S. W., and Stewart, A. L.: Inelastic Collisions between Atoms. 1. General theoretical considerations. Proc. Roy. Soc. (London), ser. A, vol. 216, no. 1127, Feb. 24, 1953, pp. 437-458.

30. Dalgarno, A., and McDowell, M. R. C.: Charge Transfer and the Mobility of H^- Ions in Atomic Hydrogen. Proc. Phys. Soc. (London), ser. A, vol. 69, 1956, pp. 615-623.

31. Popescu Iovitsu, I., and Ionescu-Pallas, N.: Resonant Charge-Exchange and the Kinetics of Ions (in Their Own Gas). Soviet-Phys.-Tech. Phys., vol. 4, no. 7, Jan. 1960, pp. 781-791.

32. Margenau, H.: On the Forces Between Positive Ions and Neutral Molecules. Phil. of Sci., vol. 8, 1941, p. 603.

33. Jahnke, E., and Emde, F.: Tables of Functions. Dover Pub., 1945.

34. Chanin, Lorne M., and Bondi, Manfred A.: Temperature Dependence of Ions Mobilities in Helium, Neon, and Argon. Phys. Rev., vol. 106, no. 3, May 1, 1957, pp. 473-479.

35. Gioumousis, George, and Stevenson, D. P.: Reactions of Gaseous Molecule Ions with Gaseous Molecules. V. Theory. Jour. Chem. Phys., vol. 29, no. 2, Aug. 1959, pp. 294-299.

36. Salop, Arthur, Pollack, Edward, and Bederson, Benjamin: Measurements of the Electric Polarizabilities of the Alkalis Using the E-H Gradient Balance Method. Phys. Rev., vol. 124, no. 5, Dec. 1961, pp. 1431-1438.

37. Maxwell, James Clerk: Dynamical Theory of Gases. Scientific Papers, vol. 2, W. D. Niven, ed., Cambridge Univ. Press, 1890, pp. 26-78.

38. Bullis, R. H., Flavin, R. K., and Meyerand, R. G., Jr.: Research on the Collision Probabilities of Electrons and Cesium Ions in Cesium Vapor. Final Rep. May 1, 1962-May 31, 1963, United Aircraft Corp., 1963.

39. Cramer, W. H.: Elastic and Inelastic Scattering of Low Velocity He^+ and Ne^+ Ions in Helium and Neon. College of Eng., Univ. Florida, 1956.

40. Cramer, W. H.: Elastic and Inelastic Scattering of Low-Velocity Ions: Ne^+ in A, A^+ in Ne, and A^+ in A. Jour. Chem. Phys., vol. 30, no. 3, Mar. 1959, pp. 641-642.

41. Cramer, W. H.: Elastic and Inelastic Scattering of Low-Velocity Ions: He^+ in Ne, Ne^+ in He, and Ne^+ in Ne. Jour. Chem. Phys., vol. 28, no. 4, Apr. 1958, pp. 688-693.

42. Bates, D. R.: Quantum Theory. I. Elements. Academic Press, 1961.

43. Irving, J., and Mullineux, N.: Mathematics in Physics and Engineering. Academic Press, 1959.

"The aeronautical and space activities of the United States shall be conducted so as to contribute . . . to the expansion of human knowledge of phenomena in the atmosphere and space. The Administration shall provide for the widest practicable and appropriate dissemination of information concerning its activities and the results thereof."

—NATIONAL AERONAUTICS AND SPACE ACT OF 1958

NASA SCIENTIFIC AND TECHNICAL PUBLICATIONS

TECHNICAL REPORTS: Scientific and technical information considered important, complete, and a lasting contribution to existing knowledge.

TECHNICAL NOTES: Information less broad in scope but nevertheless of importance as a contribution to existing knowledge.

TECHNICAL MEMORANDUMS: Information receiving limited distribution because of preliminary data, security classification, or other reasons.

CONTRACTOR REPORTS: Technical information generated in connection with a NASA contract or grant and released under NASA auspices.

TECHNICAL TRANSLATIONS: Information published in a foreign language considered to merit NASA distribution in English.

TECHNICAL REPRINTS: Information derived from NASA activities and initially published in the form of journal articles.

SPECIAL PUBLICATIONS: Information derived from or of value to NASA activities but not necessarily reporting the results of individual NASA-programmed scientific efforts. Publications include conference proceedings, monographs, data compilations, handbooks, sourcebooks, and special bibliographies.

Details on the availability of these publications may be obtained from:

SCIENTIFIC AND TECHNICAL INFORMATION DIVISION

NATIONAL AERONAUTICS AND SPACE ADMINISTRATION

Washington, D.C. 20546